Hindawi

Retraction

Retracted: The Application Effect of Remote Sensing Technology in Hydrogeological Investigation under Big Data Environment

Journal of Sensors

This article has been retracted by Hindawi, as publisher, following an investigation undertaken by the publisher [1]. This investigation has uncovered evidence of systematic manipulation of the publication and peer-review process. We cannot, therefore, vouch for the reliability or integrity of this article.

Please note that this notice is intended solely to alert readers that the peer-review process of this article has been compromised.

Wiley and Hindawi regret that the usual quality checks did not identify these issues before publication and have since put additional measures in place to safeguard research integrity.

We wish to credit our Research Integrity and Research Publishing teams and anonymous and named external researchers and research integrity experts for contributing to this investigation.

The corresponding author, as the representative of all authors, has been given the opportunity to register their agreement or disagreement to this retraction. We have kept a record of any response received.

References

[1] H. Wang, R. Yang, L. Zhao, F. Tian, and S. Yu, "The Application Effect of Remote Sensing Technology in Hydrogeological Investigation under Big Data Environment," *Journal of Sensors*, vol. 2022, Article ID 5162864, 12 pages, 2022.

Research Article

The Application Effect of Remote Sensing Technology in Hydrogeological Investigation under Big Data Environment

Honglei Wang,[1] Ronghang Yang [ID],[1] Li Zhao,[2] Feng Tian,[2] and Shizhong Yu[3]

[1]*The 7th Geological Team, Shandong Bureau of Geology and Mineral Resources Exploration and Development, Linyi, 276000 Shandong, China*
[2]*The Third Exploration Team, Shandong Coal Geology Bureau, Tai'an, 271000 Shandong, China*
[3]*Shandong Provincial Territorial Spatial Ecological Restoration Center, Jinan, 250014 Shandong, China*

Correspondence should be addressed to Ronghang Yang; 201701370103@lzpcc.edu.cn

The hydrogeological investigation is a work carried out by comprehensive utilization of various exploration methods to identify hydrogeological conditions in the target area, and develop and utilize groundwater resources. There are great differences in hydrogeological conditions in different regions. Hence, it is necessary to take exploration technology according to local conditions to master hydrogeological information as much as possible. Among them, the remote sensing (RS) technology can reflect the ground surveying and mapping results with high efficiency and precision through the analysis of satellite or aerial photographs, which is a commonly used method in the current hydrogeological investigation. According to satellite RS data, this work evaluates the distribution of groundwater levels in the study area and explores the geological and hydrogeological conditions of the groundwater system in the affected area. Firstly, the human-computer interactive interpretation method is used to analyze the topography and geomorphology conditions. Secondly, the spectral characteristic curve analysis method is used to extract the spectral characteristics of regional stratum lithology, and analyze and determine the lithology composition and structure of the aquifer. Thirdly, the single-band and multiband models of soil moisture RS estimation of groundwater level are implemented. Finally, the measured data are employed to verify and analyze the estimated value of the model. The results are in line with the actual value, and good results have been achieved.

1. Introduction

The instruments, equipments, and technical means of engineering hydrogeological investigation are developing towards automation and intelligence due to the improvement of people's understanding of the objective world and the continuous progress of science and technology [1]. On account of the traditional geological exploration industry, people continue to introduce unmanned aerial vehicles, airborne radar, laser sensors, and three-dimensional (3D) scanners. It means that the development and innovation of modern scientific and technological products are introduced into geological exploration technology [2]. With the changes of the times, the database management information system has developed rapidly. The big data processing technology has been gradually applied to the project to improve the updating efficiency of the data volume of the surveying and mapping unit and the space for collecting the data volume to store, organize, manage, and process the hydrogeological data. The big data processing method can be adopted to comprehensively analyze and evaluate hydrogeological problems and disaster risks at the project site. Moreover, it can provide technical support for disaster prevention and reduction of hydrogeological engineering geology and environmental geology. Meanwhile, building a data system of hydrogeological engineering geology and environmental geology is also conducive to effective and full management and utilization of various information resources in the future. It can also provide real and effective data for subsequent scientific research and decision-making management [3].

The current surface water resources in most parts of northern China are relatively scarce, so most water for people's production and living comes from groundwater resources. Hence, improving groundwater resources' exploration, development, and utilization are necessary for local social development [4]. The present remote sensing (RS) technology is gradually applied to the engineering survey field. It is generally defined as the technology of detecting and perceiving things and objects from a distance. Unlike other detection technologies, the coverage of RS technology is larger, the types of detection data obtained are various, and the means are diversified. Moreover, most of the detected data information is expressed through images, and the way of acquiring the detected data information is more direct and faster, making the detection time relatively short [5]. In the hydrological survey, the specific application of RS technology attaches importance to the comprehensive analysis of environmental factors related to groundwater level and RS image's data processing methods. It can comprehensively analyze the groundwater level distribution, build a scientific and reasonable groundwater level distribution model according to the principles of soil moisture, reflectance, and pixel relationship, and conduct a professional hydrogeological investigation [6].

Through the above problems, the application effect of the RS technology in the hydrogeological investigation is studied under the background of the big data environment. In this work, the human-computer interactive interpretation system GeoFrame is used based on RS satellite image data, and the spectral characteristic curve analysis method is taken to extract the spectral characteristics of the regional stratum lithology and analyze and determine the composition and structure of water-bearing lithology in the study area. Starting from the relationship between groundwater and soil moisture, based on soil moisture of RS monitoring combined with data obtained from field experiments, the correlation equation between soil moisture and groundwater level is established, and a model for evaluating the distribution of shallow underground water level is proposed. The estimation results of the implemented multiband and single-band models are verified and analyzed, and the model with good agreement between the simulation results and the actual is determined. Furthermore, it is proved that the model can estimate the distribution of the groundwater level.

2. Literature Review

Salmivaara et al. used big data technology as a storage method to retrieve massive grid data and form a spatial database of climate and other environmental data. The structured, semistructured, and unstructured geospatial data generated by the continuous production of natural resources are collected, and a geospatial data system with an integration layer and related technical components is built [7]. Chen et al. developed and opened the online index and query system SKSO pen for large-scale geospatial data, which integrates with Terra Fly geospatial database to visualize query results and data analysis [8]. Cudennec et al. believed that, as the core of geographic information services,

the spatial analysis presented two main development trends under the big data background. The first is an accurate analysis of large-scale spatial data. Due to the progress of spatial data acquisition technology, people can obtain increasingly larger space, the scale of spatial data continues to expand, and the accuracy of spatial data analysis continues to improve. The second is the real-time demand for spatial analysis services [9].

Yao et al. proposed the possibility of thermal infrared RS to evaluate groundwater by using aerial thermal infrared images and referring to massive actually collected hydrological data, topographic and geomorphic maps, Quaternary sediment distribution maps, vegetation distribution maps, and other reference materials. They successfully measured the temperature information related to groundwater [10]. Sishodia et al. selected two typical areas in China for groundwater source research. The adjustment assumption of coordination between land use structure and groundwater source was proposed based on the analysis of the change law between land development and regional environmental factors in groundwater [11]. Mohammadi found the hydrogeological conditions closely related to landform, Quaternary Geology, and neotectonics through RS images, judged the aquifer development law and various boundary types, and more accurately evaluated groundwater resources combined with geophysical prospecting results [12]. Aasen et al. extracted relevant information on the surface water system, geological structure, and aquifer properties of Tarim Basin from Landsat-MSS images. The quality, quantity, and burial depth of groundwater in Tarim Basin were investigated using the research area's geological and geomorphologic map and the precipitation and runoff text model [13]. Muchingami et al. evaluated the groundwater resources of the crystalline basement aquifer in Zimbabwe based on the vegetation distribution map and NDVI map in the study area displayed by Landset TM images [14]. In their work on drought in West Africa, Le Page et al. started the study of the relationship between groundwater and vegetation and explored the situation of groundwater resources through the analysis of the vegetation RS technology [15]. Suryanarayana et al. used two-band microwave remote sensors to establish radar and other microwave remote sensors on the basis of measured surface hydrological factors, soil dielectric constant, and soil reflectivity to study groundwater conditions in Visakhapatnam, India [16].

To sum up, relevant scholars have made certain theoretical achievements in the research of hydrogeological investigation under RS technology. Step-by-step exploration and research have confirmed that RS technology can monitor and collect data in hydrological work. Moreover, it can provide strong technical support for data investigation in hydrological work and prediction and treatment of hydrological problems. However, there are few studies on integrating RS technology in the big data environment. Some studies are based on spatial data structure, spatial database, map digitization, and automatic mapping technology. It suggests that scholars are exploring the application of RS technology in the hydrogeological investigation in the big data environment. This work is to study the hydrogeological

investigation's application effect by combining the characteristics of the two. It aims to apply advanced technology to future hydrogeological investigations.

3. Materials and Methods

3.1. Human-Computer Interactive Interpretation Method. RS technology interprets signs based on geology to identify ground targets or features through satellite images. The types of signs can be divided into direct interpretation and indirect interpretation. There are two types of interpretation methods: visual interpretation and human-computer interactive interpretation. This time, the human-computer interactive interpretation method is used to investigate the distribution of groundwater levels in the study area. Interactive interpretation is often translated as human-computer interactive interpretation. As the name implies, it is the work process of comprehensive interpretation of geological and geophysical data by the interpreter with the assistance of computers. The interpreter issues an instruction in the interactive interpretation workstation, and the computer displays the corresponding execution result of the instruction. Interaction means that the computer is in the working state, and the operator waits for the response of the issued instruction in front of the computer terminal. The shorter the waiting time is, the better the computer performance is. If the computer's response is inappropriate or unsatisfactory, the operator can modify the instruction at any time until it is satisfied. This process is realized by the computer and the operator in the form of dialogue. In other words, the response of the interactive system is fast, and the interpreter can immediately complete any operation within the functional scope of the interpretation system [14]. Figure 1 demonstrates the advantages of human-computer interactive interpretation over manual interpretation:

The interactive interpretation of geological data is currently in the stage of popularization and in-depth development. China's present dominant interactive interpretation system is the GeoFrame interpretation system. It is mainly adopted for comprehensive analysis and interpretation of seismic, well logging, geological, and reservoir simulation data in exploration and development [15]. After receiving an interpretation project, all kinds of data used for interactive interpretation must be collected, including the geological and geomorphic results data of the interpretation work area, the measurement curves of all water levels, and the geological stratification data. Then, the data management software of the interactive interpretation system is employed to store the above-mentioned relevant data in a specific database. The database in the interpretation system refers to a collection of interrelated data reasonably stored on the computer storage device. Usually, each work area corresponds to a database. It is equivalent to a full-time and responsible work area data keeper, who can access any data anytime. In addition to the original data, the database also reserves the position and space for the later interpreted data of reflection layer and fault and various image data. It means that the database or data management system keeps all data files throughout the interpretation process [16]. Figure 2 details a flowchart of its startup operation:

Human-computer interactive interpretation unifies images, graphics, and data. It can be adopted to superimpose various images and graphics according to the requirements of interpreters and verifiers in the verification of the information recognition process and interpretation results. Then, the required statistical data can be obtained simultaneously after the interpretation to achieve the unification of images, graphics, and data. Now, the application scope of human-computer interactive interpretation is expanding with the rapid progress of digitalization [17]. Figure 3 is the main work steps of interactive interpretation summarized after understanding the GeoFrame interactive interpretation system:

In this work, GeoFrame is used to interpret and analyze the RS images of water bodies. Since water bodies have obvious spectral characteristics among various types of ground objects, when analyzing and extracting relevant information, selecting the most suitable synthetic band can achieve twice the result with half the effort. For example, in the visible light band, the reflectivity of relatively clear and clean water decreases rapidly as the wavelength increases (blue light-red light). In the blue-green band ($0.04 \sim 0.6 \, \mu$m), the reflectivity is relatively large, and the interpretation effect of the TM1 and TM2 bands is the best. For topics related to the analysis of surface vegetation, the interpretation effect of the TM4 band is better; while the reflectivity of the red-infrared band ($0.06 \sim 2.5 \, \mu$m) is greatly weakened, and the infrared band is basically completely absorbed. Therefore, TM3 and TM7 bands are selected to cover more comprehensive information. Here, various analysis elements and influence conditions are integrated, and TM7, 4, and 3 bands are chosen to analyze the distribution of groundwater levels [18].

3.2. RS Technology. In 1960, the American scholar E. L. Pruiet called the technology of obtaining the images or data of the detected targets by photographing and nonphotographing "RS" to comprehensively summarize the technologies and methods of detecting targets. This term was formally adopted at the Environmental Science Symposium held by the University of Michigan and other units in 1962. RS detects the target, obtains the information of the target, and then processes the acquired information to realize the positioning, qualitative, or quantitative description of the target [19]. The current remote sensing geological exploration technology has been applied to practical projects. Figure 4 displays the primary application areas. This work uses RS to investigate the hydrogeological conditions affecting the groundwater system in the study area. Then, through the RS monitoring model of groundwater level distribution, combined with Landsat5 thematic mapper (TM) RS satellite image data, the distribution of regional groundwater levels is analyzed and interpreted. For the extraction and interpretation of this information, the following exploration are carried out. By using the groundwater level data of the measured sample points in the study area, the estimation results of the single-band and multiband models are verified and analyzed, and the estimation model with good agreement between the simulation results and the actual is
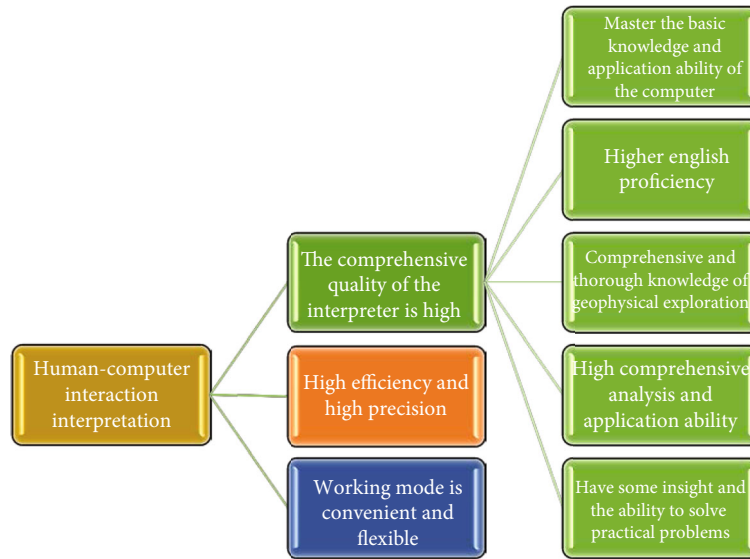
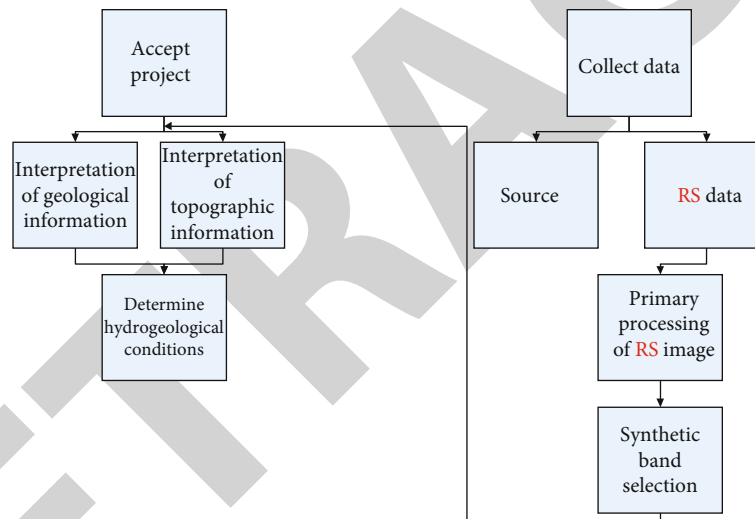Figure 1: Human-computer interactive interpretation technology.

Figure 2: Operation flow of GeoFrame system.

determined. Furthermore, the distribution of shallow groundwater levels in the study area is estimated by this model. RS has diverse classifications from different angles [20]. Here are examples of various RS types classified by RS platform and sensor detection band. Figure 5 presents the details:

The spatial resolution and spectral resolution of RS images of optical systems are contradictory. Generally, under a certain signal-to-noise ratio, the improvement of spectral resolution is at the expense of spatial resolution. Fusing low-resolution multispectral images with high-resolution panchromatic band images can improve the multispectral data's spatial resolution. Thereby, various RS image fusion algorithms have been rapidly developed and applied [21]. Figure 6 portrays a schematic diagram of electromagnetic radiation received by the remote sensor.

Since different RS images have diverse representation capabilities of ground objects and various image characteristics, it is required to select an appropriate RS data type when interpreting. After selecting the RS data type, it should also be considered to select a suitable interpretation band according to the spectral characteristic curve of the ground object. Under the premise of fully investigating the basic conditions of the study area, this work analyzes the distribution of groundwater levels in the study area based on RS data and field experimental observation data. The seven-band images of the TM of the Landsat 5 satellite launched by NASA are selected for analysis, and the applicable bands are selected according to the spectral characteristic curve of the existing.

3.3. Spectral Characteristic Curve Analysis. Gram-Schmidt (GS) transform is adopted in this work to make the fused image fidelity better and the results more practical. Orthogonalization of matrix or multidimensional images can eliminate redundant information, and the calculation process is
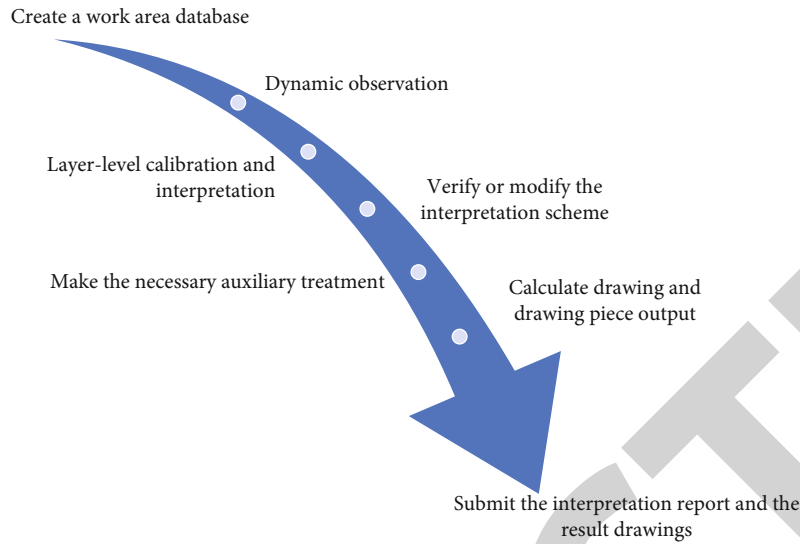
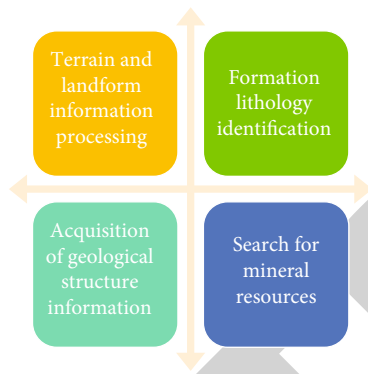Figure 3: Working steps of interactive interpretation.

Figure 4: Application field of RS geological survey.

simple. Multispectral images are adopted to simulate panchromatic bands. There are two simulation methods:

(1) The multispectral band with the low spatial resolution is simulated according to the spectral response function with a certain weight W_i. It refers to the simulated panchromatic band gray value:

$$P = \sum_{i-1}^{n} W_i * B_i. \quad (1)$$

In equation (1), B_i denotes the i-th band gray value of the multispectrum.

(2) The panchromatic band image is blurred, and then a subset is taken. Next, the image is reduced to the same size as the multispectral image. The simulated panchromatic band is converted as GS_1 in the processing of the next step. The first component in the GS transform does not change after the simulated panchromatic band is adopted to exchange with the

panchromatic band. Hence, the spectral information of RS data is less distorted and has higher accuracy

The simulated panchromatic band is taken as GS_1 to perform GS transformation on the simulated panchromatic band and multispectral band. The algorithm is modified during GS transformation. The specific modification is as follows. The first T-1 GS component constructs the T-th GS component, that is:

$$GS_T(i, j) = [B_T(i, j) - u_T] - \sum_{i-1}^{T-1} \varphi(B_T, GS_i) * GS_i(i, j), \quad (2)$$

$$u_T = \frac{\sum_{j-1}^{C} \sum_{i-1}^{R} B_T(i, j)}{C * R}, \quad (3)$$

$$\varphi(B_T, GS_i) = \left[\frac{\sigma(B_T, GS_i)}{\sigma(GS_i, GS_i)^2} \right], \quad (4)$$

$$\sigma_T = \sqrt{\frac{\sum_{j-i}^{C} \sum_{i-1}^{R} [B_T(i, j) - u_T]}{C * R}}. \quad (5)$$

In equation (2), GS_T represents the T-th component generated after GS transformation. B_T is the T-th band of the original multispectral image. u_T donates the mean value of the gray value of the T-th original multispectral band image. In equation (3), B_T expresses the original multispectral T-th band. In equation (4), GS_i refers to the i-th component generated after GS transformation. In equation (5), u_T stands for the average of the grayscale values of the T-th original multispectral image.

Adjusting the statistical value of the panchromatic band to match GS_1 can generate the modified panchromatic band. This work is conducive to preserving the spectral characteristics of the original multispectral images. The modified panchromatic band is replaced with the first component after GS transform to generate a new dataset. A
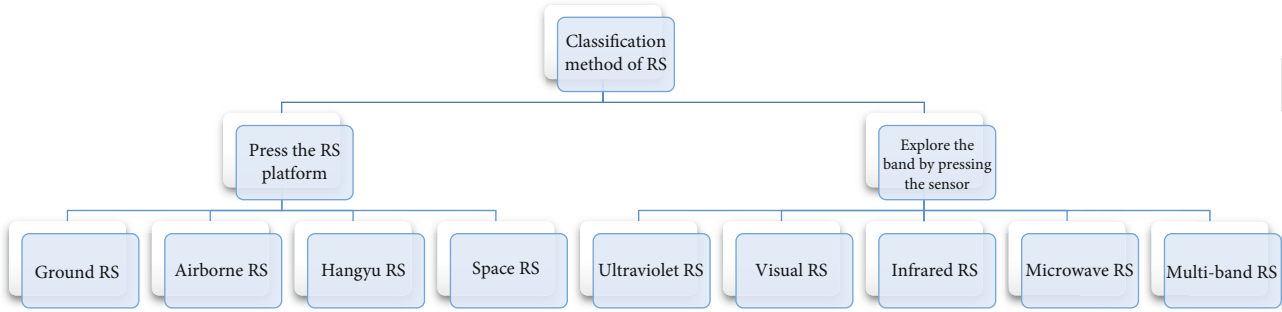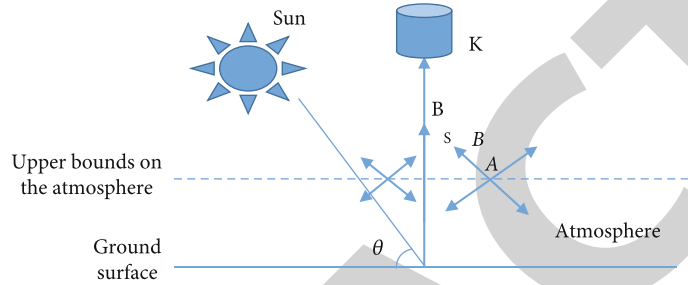
Figure 5: Different classifications of RS.

Figure 6: Schematic diagram of remote sensor receiving electromagnetic radiation.

multispectral image with enhanced spatial resolution can be generated by performing inverse GS inverse transform on the new dataset. The equation of GS inverse transformation is as follows:

$$\widehat{B_T}(i,j) = [GS_T(i,j) + u_T] + \sum_{i-1}^{T-1} \varphi(B_T, GS_i) * GS_i(i,j). \quad (6)$$

According to the analysis and interpretation results of the topographic and geomorphic types in the research area, the different types of areas are classified, analyzed, and interpreted to identify the stratum lithology. A lithologic spectrum library in the study area is created to facilitate the analysis and identification of the lithologic characteristics of various types of strata. According to the previous research results, the stratum lithology in the study area is mainly sandstone and mudstone, and the surface layer is mostly sandy soil and sandy loam, with a clay layer. Figures 7 and 8 are typical stratum lithologic spectral curve characteristics:

In Figures 7 and 8, the spectral characteristics of different types of rocks are quite distinct. The differences are mainly reflected in the reflectance of the spectrum and the position and depth of the characteristic absorption peak, which are also the basis for lithologic mineral identification. The waveforms of the same type of rocks are similar and the characteristic absorption peaks are consistent. However, due to different lithological purity, rocks' spectral reflectance, and characteristic absorption intensity will change accordingly. According to the difference of the reflection spectrum of the rock, it is identified that the lithology of the experimental area is dominated by sandstone and mudstone, and the surface layer is mostly sandy soil and sandy loam. Since the Quaternary stratum is mostly composed of loam, sand,

gravel, sand gravel, etc., it is easy to host groundwater. Therefore, the groundwater area in the study area generally occurs in the Quaternary strata. Moreover, half of the RS water-seeking information is close to the fault structure, and it is also easy to appear on the stratum uplift. Therefore, it is necessary to combine the specific formation conditions.

Three points are selected for the removal of the reference spectrum and pixel continuum: the absorption center and the points on both sides of the absorption center. To homogenize the noise on the continuum, several bands on both sides of the absorption center can be selected to remove the continuum by the following division:

$$L_c = \frac{L(\lambda)}{C_l(\lambda)}, \quad (7)$$

$$O_c(\lambda) = \frac{o(\lambda)}{C_0(\lambda)}. \quad (8)$$

$L(\lambda)$ denotes the spectrum as a function of wavelength λ; O illustrates the pixel spectrum; C_l refers to continuum spectrum; C_0 means the continuous spectrum of the pixel. An additional constant K is adopted to increase the contrast of the reference spectrum:

$$L_c' = \frac{L_c + K}{1.0 + K}. \quad (9)$$

L_c' indicates the adjusted continuum removal spectrum, which best fits the observation spectrum.

3.4. RS Estimation of the Distribution of Groundwater Level. Different soils have slightly various constants due to different soil types. On account of the statistical and regression
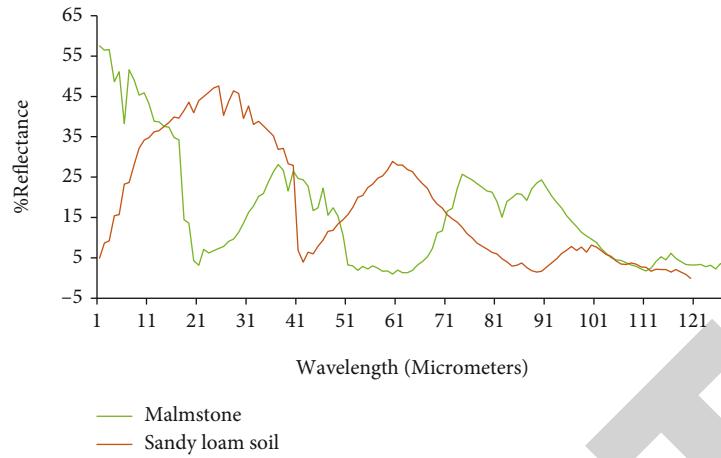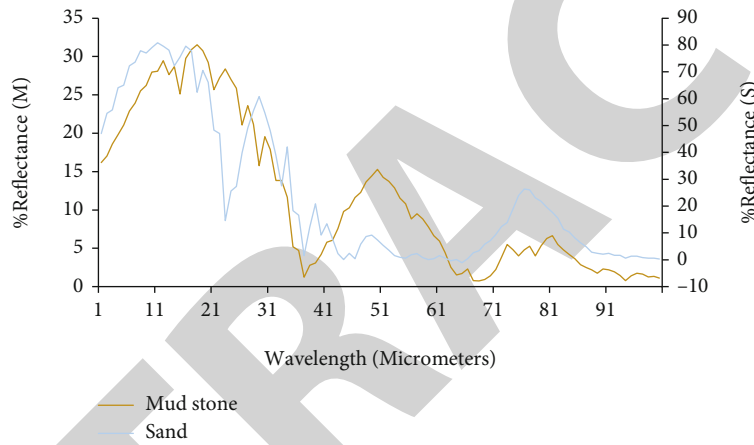
FIGURE 7: Spectral curve 1.

FIGURE 8: Spectral curve 2.

analysis results of the measured data in the study area, the relationship between reflectance and water content is established. The correlation coefficients of the regression analysis of various soils in the study area are generally 0.92 to 0.98 [22]. Therefore, the average value of the RS model of several types of soil moisture in this area was taken to analyze the soil moisture status:

$$W_i = 91.70 - 42.91 \bullet \log R_{i\pm}1. \tag{10}$$

In equation (10), W_i is the percentage of soil moisture obtained in the i-band.

The distribution of water in the capillary can be written as an equation (11):

$$W^2(y) = A + By, \max(0, H - H_m) \leq y \leq H_m. \tag{11}$$

In equation (11), H means the depth of groundwater, and H_m indicates the depth that can rise from the groundwater-soil contact surface to the capillary.

H_m is related to the physical and chemical properties of the soil. The same soil type has a similar H_m value. Different soil types have diverse heights that groundwater can rise to

the capillary. The constants A and B are determined by the following 3 boundary conditions:

(1) At the contact surface between soil and groundwater, $y = H$, the maximum value of the soil moisture is $W_{\max}$;

(2) When the groundwater can rise to the height of the capillary, $y = H - H_m$, the minimum value of soil moisture is $W_{\min}$;

(3) At the soil-atmosphere contact surface, $y = 0$, and the soil moisture is W0. Boundary conditions (1) and (2) are substituted into equation (11), as follows:

$$A = W^2_{\max} W^2_{\max} W^2_{\min} \frac{H}{H_m}, \tag{12}$$

$$B = \frac{W^2_{\max} W^2_{\min}}{H_m}. \tag{13}$$

Boundary condition (2) is replaced by (3), which

transforms to:

$$A = W_0^2, B = \frac{W_{\max}^2 W_0^2}{H}.\qquad(14)$$

The multiyear average precipitation in the study area is 389.34 mm, but the multiyear average evaporation is as high as 1411.49 mm. The soil in this area is mostly aeolian sandy soil developed on fixed and semifixed dunes, and the surface soil moisture is small, so the correlation between the groundwater level and the surface soil moisture is very small. Thereby, equation (14) does not need to be considered here.

When the parameters $W_{\max}$, $W_{\min}$, H_m, and the effective depth of soil moisture of RS monitoring are determined, the groundwater level in the study area can be estimated by equation (11). However, for the Landsat5 satellite, the effective depth of RS monitoring of soil moisture is limited to very shallow soil layers near the surface, and the effective

depth of monitoring is generally 0.10 m, and the relative relationship between shallow soil moisture and groundwater level is not stable. Due to the limitation of the effective depth of groundwater level monitoring by RS, this analysis is limited to areas with shallow soil and good water-richness [23].

If d is the effective depth of the monitored soil moisture, let $y = d$. W_d represents soil moisture at depth d. From equations (11), (12), and (13), the relationship equation (15) of soil moisture and groundwater level can be obtained:

$$H = d + H_m \frac{W_{\max}^2 - W_d^2}{W_{\max}^2 - W_{\min}^2}.\qquad(15)$$

By using equations (10), (11), and (15), the following single-band and multiband models for RS monitoring of groundwater levels can be obtained, as denoted in equations (16) and (17):

$$H_i = d + H_m \frac{W_{\max}^2 - [76.3 - 42.91\bullet\log(0.996B_i - 42.05)]^2}{W_{\max}^2 W_{\min}^2},\qquad(16)$$

$$H_{432} = d + H_m \frac{W_{\max}^2 - [76.3 - 42.91\bullet\log(0.6968B_2 + 0.5228B_3 - 0.2237B_4 + 20.26/1.089 - 0.00579B_4 + 0.003308B_2 + 0.002482B_3 - 18]^2}{W_{\max}^2 W_{\min}^2}.$$
$$(17)$$

In equations (16) and (17), H_i is the buried depth of groundwater level estimated by the i-th band of TM;

By analyzing the estimation formulas of single-band and multiband, if the hydrological constants $W_{\max}$, $W_{\min}$, H_m are known, and the effective depth d of soil moisture monitoring by RS is determined, the groundwater level can be quantitatively determined [24].

4. Results

Correlation analysis is conducted on the groundwater level estimated by the single-band and multiband groundwater level monitoring models and the measured groundwater level. Figures 9–12 present the comparison between the groundwater monitoring value and the measured data:

Figure 9 suggests that the maximum error between the monitoring value of groundwater level and the actual value in the third band is 0.8, which appears at the A10 sample point. The minimum error value is 0, which appears at sample points A3 and A4. Excluding the maximum and minimum values, the error value is basically maintained within 0.4. The error value is within the allowable error range. It suggests that the spectral characteristic curve can basically reflect the situation of groundwater. The appropriate model is chosen for future hydrogeological investigation by comparing the multiband groundwater level monitoring.

Figure 10 suggests that the maximum error between the monitoring value groundwater level and the actual value of

the fourth band is 0.8, which appears at the A10 sample point. The minimum error value is 0, which appears at A4, A5, and A8 sample points. Excluding the maximum and minimum values, the error value is basically maintained within 0.3. The error value is within the allowable error range. It proves that the spectral characteristic curve can basically reflect the groundwater situation, which is more accurate than the response of the third band. The appropriate model is selected for future hydrogeological investigation by comparing the multiband groundwater level monitoring.

Figure 11 suggests that the maximum error between the monitoring value and the actual value of the groundwater level in band 7 is 0.9, which appears at the A10 sample point. The minimum error value is 0, which appears at sample points A3, A4, and A6. Excluding the maximum and minimum values, the error value is basically kept within 0.4. The error value is within the allowable error range. It reveals that the spectral characteristic curve can basically reflect the groundwater situation. However, the prediction accuracy is slightly worse than that of the first two bands. The appropriate model is selected for future hydrogeological investigation by comparing the multiband groundwater level monitoring.

Figure 12 details that the error range between the multiband groundwater level monitoring value and the actual value is relatively stable and can be maintained within 0.4. Moreover, the error values are generally quite low, illustrating that multiband is more suitable for groundwater level monitoring than single-band. Meanwhile, the correlation
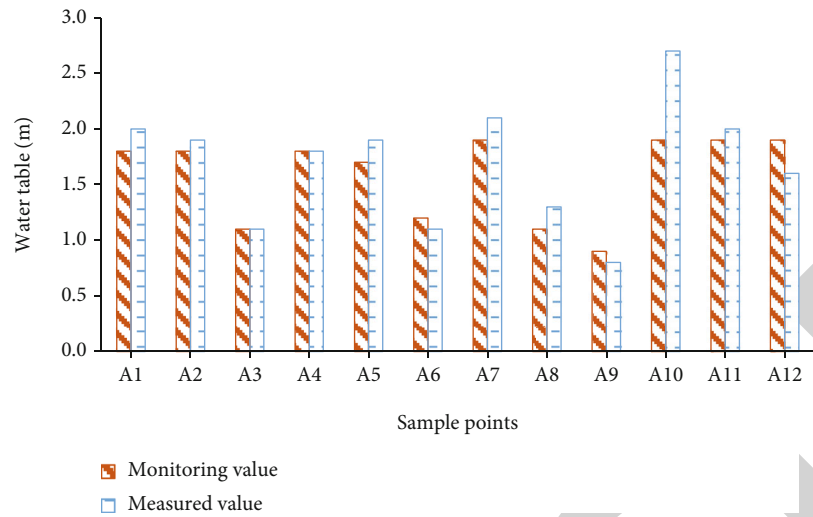
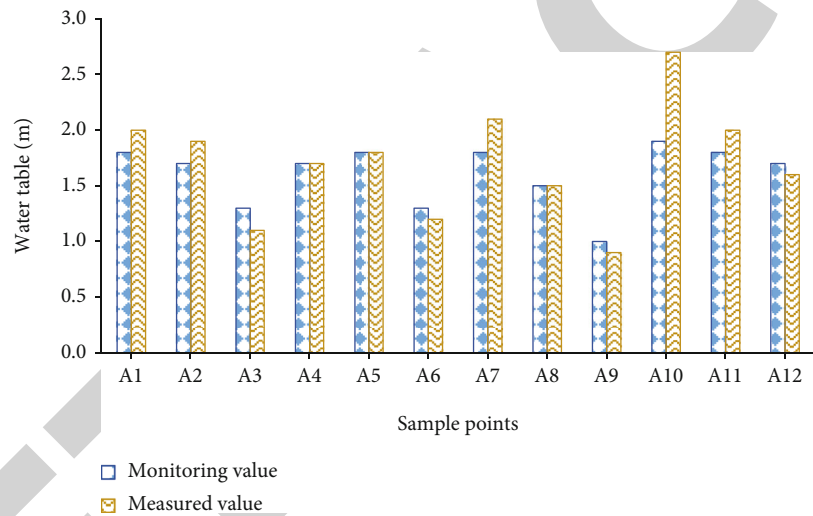FIGURE 9: The comparison of groundwater level values in band 3.

FIGURE 10: The comparison of groundwater level values in band 4.
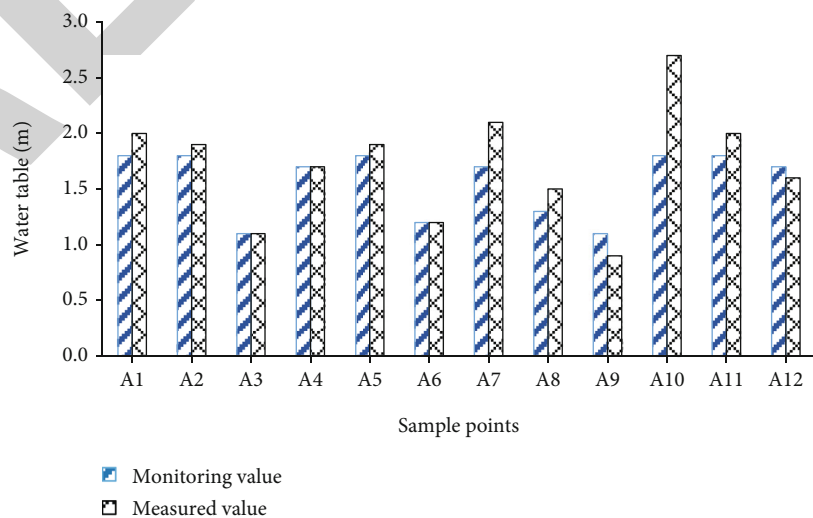

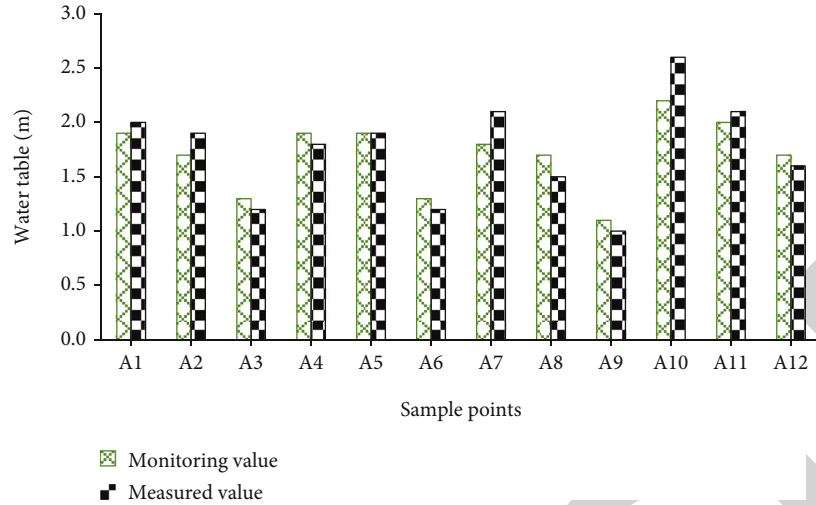FIGURE 11: The comparison of groundwater level values in band 7.

FIGURE 12: The comparison of multiband groundwater level values.

coefficient between the groundwater level estimated by the single-band groundwater level monitoring model and the measured groundwater level is generally lower than the correlation coefficient between the groundwater level estimated by the multiband groundwater level monitoring model and the measured groundwater level. It further confirms that the multiband model is better than the single-band model to be better applied to hydrogeological investigation. Table 1 exhibits the summary of the data obtained from the above histogram:

Table 1 shows that the average error values of the three single bands are 0.19, 0.18, and 0.20, respectively, and the average error value of the multiband is 0.15. In comparison, the multiband error value is the smallest, and the error values of the three single bands are equal. It illustrates that the multiband survey of groundwater levels is more accurate. Meanwhile, the correlation coefficients between the groundwater level estimated by the third, fourth, and seventh single-band groundwater level monitoring models and the measured groundwater level are 0.87, 0.83, and 0.89, respectively. The correlation coefficient between the groundwater level estimated by the second, third, and fourth multiband groundwater level monitoring models and the measured groundwater level is 0.93. In the estimation model, the multiband model is better than the single-band model, which can better reflect the groundwater level. The distribution of groundwater monitored by the model can accurately reflect the actual situation of the groundwater level, and the research results are basically in line with reality. Therefore, it is feasible to use the multiband model to monitor the groundwater level.

5. Discussion

Zhang et al. established a lithologic spectral library in the research area with the assistance of ENVI software based on the research area's interpretation and analysis of topography and geomorphology. According to different lithologic spectral characteristic curves, they analyzed the spectral

TABLE 1: The comparison of error value and correlation coefficient.

Different bands	Mean error	Correlation coefficient
Band 3	0.19	0.87
Band 4	0.18	0.83
Band 7	0.20	0.89
Multiband	0.15	0.93

characteristic differences and influence characteristics of different lithologic stratigraphic units in the research area. The lithologic and stratigraphic interpretation was conducted using the manual visual interpretation method. The strata's lithologic structure in the study area was basically mastered, and the comprehensive geological histogram of the study area was prepared [25]. Here, after extracting the characteristic spectral curve, the monitoring value of groundwater level in single-band and multiband are compared with the actual value. The single-band and multiband RS monitoring models of groundwater level distribution have been implemented, paving the way for the effective monitoring of groundwater levels through analyzing soil moisture status by RS technology. Thus, it is concluded that the spectral characteristic curve of RS technology can be employed to accurately measure the groundwater level landmark, which provides good help to the hydrogeological investigation.

Xu used human-computer interactive geomorphological interpretation technology to study submarine landslides. The results demonstrate that this technique can reduce the bias of subjective factors on interpretation. More importantly, it can fully mine the hidden information that is not easy to find in manual interpretation, improve the accuracy and scientificity of interpretation, and avoid the error caused by manual interpretation [26]. The application of human-computer interactive interpretation technology in the hydrogeological investigation suggests that the GeoFrame system used by some enterprises has certain advantages in terrain and geomorphology analysis. The 3D geological exploration

improvement will inevitably promote the rapid development of human-computer interactive interpretation technology. It is only possible to understand the structure of subtle and complex small faults when fully using the drilling and production, well logging, geological data, and imaging technology of 3D geological data, together with human experience and wisdom.

6. Conclusion

Under the background of a big data environment, RS technology is adopted to analyze the spectrum of the study area, and the information of hydrogeological factors affecting and restricting the groundwater resource system is obtained. Meanwhile, a mathematical model for effectively detecting groundwater resources by RS images is implemented through the RS - spectral fusion research method and the actual situation of the study area. The distribution of groundwater levels in this area is further analyzed, and the stratum lithology and structure of the area are basically mastered. The comprehensive geological column comparison map of the study area is made. The single-band and multiband RS monitoring models of groundwater level distribution have been constructed. It provides a practical theory for future hydrogeological investigation and proves that the method of monitoring and evaluating groundwater distribution using a multiband model is feasible. Meanwhile, this experiment also has some shortcomings. In the process of human-computer interactive interpretation, the accuracy of interpretation results may be affected due to the lack of knowledge system and experience. There is a lack of more effective references and comparisons in lithologic information extraction due to less experimental work in the process of water information spectral extraction and the lack of a lithologic distribution map in the research area. It affects the accuracy of lithologic classification result evaluation. In the analysis of groundwater level distribution, the impact of terrain factors, air temperature, wind speed, and other factors on soil moisture is not considered, resulting in a decrease in the accuracy of the estimated value.

Data Availability

The data used to support the findings of this study are available from the corresponding author upon request.

Conflicts of Interest

The authors declare no conflicts of interest.

References

[1] A. Bukhari, H. Hendrayana, and H. Setiawan, "Preliminary conceptual model of hydrogeological system in the Raimanuk and its surrounding area on the Timor Island," *IOP Conference Series: Earth and Environmental Science*, vol. 930, no. 1, article 012058, 2021.

[2] F. M. D'Affonseca, M. Finkel, and O. A. Cirpka, "Combining implicit geological modeling, field surveys, and hydrogeological modeling to describe groundwater flow in a karst aquifer," *Journal*, vol. 28, no. 8, pp. 2779–2802, 2020.

[3] M. Nursaputra, R. A. Barkey, S. Rijal, C. Anila, and M. F. Mappiasse, "The direction of land-use for hydrology balance and development of low-carbon emissions in the Jenelata catchment area," *IOP Conference Series: Earth and Environmental Science*, vol. 681, no. 1, p. 14, 2021.

[4] Y. S. Xu, J. S. Shen, A. N. Zhou, and A. Arulrajah, "Geological and hydrogeological environment with geohazards during underground construction in Hangzhou: a review," *Arabian Journal of Geosciences*, vol. 11, no. 18, pp. 1–18, 2018.

[5] Y. Huang, Z. X. Chen, Y. U. Tao, X. Z. Huang, and X. F. Gu, "Agricultural remote sensing big data: management and applications," *Journal of Integrative Agriculture*, vol. 17, no. 9, pp. 1915–1931, 2018.

[6] A. Alamanos, A. Rolston, and G. Papaioannou, "Development of a decision support system for sustainable environmental management and stakeholder engagement," *Hydrology*, vol. 8, no. 1, p. 40, 2021.

[7] A. Salmivaara, S. Launiainen, J. Perttunen et al., "Towards dynamic forest trafficability prediction using open spatial data, hydrological modelling and sensor technology," *Forestry: An International Journal of Forest Research*, vol. 93, no. 5, pp. 662–674, 2020.

[8] L. Chen and L. Wang, "Recent advance in earth observation big data for hydrology," *Big Earth Data*, vol. 2, no. 1, pp. 86–107, 2018.

[9] C. Cudennec, H. Lins, S. Uhlenbrook, and B. Arheimer, "Editorial – towards FAIR and SQUARE hydrological data," *Hydrological Sciences Journal*, vol. 65, no. 5, pp. 681-682, 2020.

[10] H. Yao, R. Qin, and X. Chen, "Unmanned aerial vehicle for remote sensing applications—a review," *Remote Sensing*, vol. 11, no. 12, p. 1443, 2019.

[11] R. P. Sishodia, R. L. Ray, and S. K. Singh, "Applications of remote sensing in precision agriculture: a review," *Remote Sensing*, vol. 12, no. 19, p. 3136, 2020.

[12] B. Mohammadi, "Application of machine learning and remote sensing in hydrology," *Sustainability*, vol. 14, no. 13, p. 7586, 2022.

[13] H. Aasen, E. Honkavaara, A. Lucieer, and P. Zarco-Tejada, "Quantitative remote sensing at ultra-high resolution with UAV spectroscopy: a review of sensor technology, measurement procedures, and data correction workflows," *Remote Sensing*, vol. 10, no. 7, p. 1091, 2018.

[14] I. Muchingami, C. Chuma, M. Gumbo, D. Hlatywayo, and R. Mashingaidze, "Review: approaches to groundwater exploration and resource evaluation in the crystalline basement aquifers of Zimbabwe," *Hydrogéologie*, vol. 27, no. 3, pp. 915–928, 2019.

[15] M. Le Page and M. Zribi, "Analysis and predictability of drought in northwest Africa using optical and microwave satellite remote sensing products," *Scientific Reports*, vol. 9, no. 1, p. 1466, 2019.

[16] C. Suryanarayana and V. Mahammood, "Groundwater-level assessment and prediction using realistic pumping and recharge rates for semi-arid coastal regions: a case study of Visakhapatnam city, India," *Hydrogéologie*, vol. 27, no. 2, pp. 249–272, 2019.

[17] P. Gao, "Key technologies of human–computer interaction for immersive somatosensory interactive games using VR technology," *Soft Computing*, vol. 26, pp. 10947–10956, 2022.

[18] Y. Shu, C. Xiong, and S. Fan, "Interactive design of intelligent machine vision based on human-computer interaction mode," *Microprocessors and Microsystems*, vol. 75, article 103059, 2020.

[19] A. Søgaard Neilsen and R. L. Wilson, "Combining e-mental health intervention development with human computer interaction (HCI) design to enhance technology-facilitated recovery for people with depression and/or anxiety conditions: an integrative literature review," *International Journal of Mental Health Nursing*, vol. 28, no. 1, pp. 22–39, 2019.

[20] R. Gunderson, "Human–computer interaction research needs a theory of social structure: the dark side of digital technology systems hidden in user experience," *Human Studies*, vol. 2022, pp. 1–22, 2022.

[21] T. Vuletic, A. Duffy, L. Hay, C. McTeague, G. Campbell, and M. Grealy, "Systematic literature review of hand gestures used in human computer interaction interfaces," *International Journal of Human-Computer Studies*, vol. 129, pp. 74–94, 2019.

[22] Y. Zhong, A. Ma, Y. Soon Ong, Z. Zhu, and L. Zhang, "Computational intelligence in optical remote sensing image processing," *Applied Soft Computing*, vol. 64, pp. 75–93, 2018.

[23] M. Amani, A. Ghorbanian, S. A. Ahmadi et al., "Google earth engine cloud computing platform for remote sensing big data applications: a comprehensive review," *IEEE Journal of Selected Topics in Applied Earth Observations and Remote Sensing*, vol. 13, pp. 5326–5350, 2020.

[24] A. Asokan and J. Anitha, "Change detection techniques for remote sensing applications: a survey," *Earth Science Informatics*, vol. 12, no. 2, pp. 143–160, 2019.

[25] G. Zhang, S. Lu, and W. Zhang, "CAD-Net: a context-aware detection network for objects in remote sensing imagery," *IEEE Transactions on Geoscience and Remote Sensing*, vol. 57, no. 12, pp. 10015–10024, 2019.

[26] W. Xu, "Toward human-centered AI," *Interactions*, vol. 26, no. 4, pp. 42–46, 2019.